Eur. Phys. J. B **26**, 159–166 (2002)
DOI: 10.1140/epjb/e20020077

THE EUROPEAN PHYSICAL JOURNAL B
EDP Sciences

Calculation of optical properties within the Local Density Approximation to Density Functional Theory: application to palladium

P. Monachesi[1,a], R. Capelli[2], and R. Del Sole[2]

[1] Dipartimento di Fisica - Universitá dell'Aquila, and Istituto Nazionale per la Fisica della Materia, 67010 L'Aquila, Italy
[2] Dipartimento di Fisica - Universita' di Roma, "Tor Vergata", and Istituto Nazionale per la Fisica della Materia, 00133 Roma, Italy

Received 4 September 2001

Abstract. We calculate the optical functions of Pd using the *ab initio*, all-electron Full Potential Linear Muffin Tin Orbital method within the framework of the Density Functional Theory in the Local Density approximation. We test, in the case of Pd, the convergence of the dielectric function and energy loss function in different energy ranges *vs.* the completeness of the basis and give a quantitative estimate of the accuracy. The present approach opens the possibility of extending the energy range where the optical functions can be calculated with good accuracy without increasing the computational effort.

PACS. 71.15.Mb Density functional theory, local density approximation, gradient and other corrections – 78.20.-e Optical properties of bulk materials and thin films – 78.66.Bz Metals and metallic alloys

1 Introduction

All-electron *ab initio* methods for the calculation of the electronic properties of solids are based on the Density Functional Theory (DFT) devised by Hohenberg, Kohn and Sham [1]. This theory relies on the ground state electronic density for the construction of the total potential appearing in the Kohn-Sham (KS) equations. The exchange-correlation part of the potential is usually calculated within the Local Density Approximation (LDA), yielding reliable ground state properties. This is demonstrated by the successful determination of structural, equilibrium and elastic properties of a very large number of elemental and compound crystals [2]. However, being DFT a ground-state theory, the eigenvalues and eigenvectors resulting from the solution of the Kohn-Sham equations do not represent the physical energy spectrum and the electronic states of the system. Corrections to this approach are, in principle, necessary when one tries to describe properties that involve excited states.

Nevertheless, it is a widespread practice to adopt DFT-LDA to describe excited states, assuming that the Kohn-Sham solutions are good approximations to the true quasi-particles. In the case of semiconductors, the main shortcoming of this approximation is an almost constant underestimation of the gaps between filled and empty states [3]. In the case of metals, it is expected to be much better. With this cautions in mind it is possible to interpret, by *ab initio* DFT-LDA, experimental results involving also excited states, as, for instance, optical properties.

First principle electronic structure calculations in intermetallic systems allowed indeed to interpret the structures observed in the reflectivity spectrum of Yb ternaries on the basis of the energy band scheme [4] and to calculate the conductivity spectrum in PrSb [5] quite satisfactorily. In the following, we will assume that the linear optical response of a transition metal can be well described within DFT-LDA and we address, instead, the problem of the accuracy needed in these calculations, taking the optical properties of Pd as a test case. Our calculations are performed with a code devised to be the Full Potential (FP) version [6] of the Linear Muffin Tin Orbital (LMTO) method [7]. This can be considered one of the most powerful codes for *ab initio* electronic and optical calculations. Its very flexible basis of muffin-tin orbitals allows fast converging and accurate calculations of bulk and surface ground state and optical properties [8]. We will show below that the full-potential LMTO approach is able to give a good account of optical properties in a wide energy range (up to 70 eV), provided a well converged, relatively extended, basis is used.

The theory of the optical response of solids to an electromagnetic perturbing field, developed in the random-phase approximation [9], leads to the microscopic dielectric function [10] $\epsilon_{\mathbf{G},\mathbf{G}'}(\mathbf{q},\omega)$. Here $\mathbf{q}$ and ω are the wave vector and frequency of the electromagnetic field and $\mathbf{G}$, $\mathbf{G}'$ are reciprocal-space vectors of the crystal. The $\mathbf{q} \to 0$ limit of $\epsilon_{\mathbf{G},\mathbf{G}'}(\mathbf{q},\omega)$ allows to write the macroscopic dielectric function as a leading term in $\mathbf{G}, \mathbf{G'}$=0 plus a

[a] e-mail: patrizia.monachesi@roma2.infn.it

more complex term depending on $\mathbf{G}, \mathbf{G'} \neq 0$ representing the so-called *local field* correction [11]. Restricting oneself to the leading term of the macroscopic dielectric function allows to write the optical linear response as $\epsilon(\omega) = \epsilon_{00}(0, \omega)$, whose imaginary part, $\epsilon_2(\omega)$ may be calculated from the matrix elements of the momentum operator among unoccupied and occupied crystal electronic states (Kohn-Sham eigenstates) [12]. The real part, $\epsilon_1(\omega)$, is then obtained by the Kramers-Kronig relations that require the knowledge of $\epsilon_2(\omega)$ over a very large (in principle infinite) frequency range. The point we make here is that the reliability of the calculated $\epsilon_2(\omega)$ depends critically on the completeness of the basis chosen to expand the electron wave functions. To be more precise, the truncation of the basis determines, as a first consequence, the energy range where the dielectric function may be considered accurate. This aspect has been discussed in detail for the FP-LMTO calculation of the dielectric function in non metallic systems like Si, Ge, GaAs under pressure [13] and in graphite [14]. In the present paper we will focus on the electron energy loss (EELS) function of Pd showing that the completeness of the basis must be substantially increased with respect to total energy calculations, to obtain accurate results. Local field effects would increase substantially the computational effort; on the other hand, they have been shown to be very small in the case of copper [15]. They are therefore neglected throughout in the present calculations.

Pd is a transition metal with a potential applicative interest. Measurement of the dielectric function [16,17], conductivity, reflectivity [18] and electron energy loss [19,20] are available. Theoretical calculations of optical spectra have been performed some years ago by Uspenskii and co-workers [21], with the LMTO method in the atomic-sphere approximation, with poor agreement with the experiments. Recently different approaches have been used to improve the calculations of the optical functions [22,23]. The former approach [22] consists in an all-electron method within DFT-LDA, that includes a very large number ($\simeq$500) of unoccupied Kohn-Sham levels for the evaluation of the density response. The resulting EELS spectrum of Pd calculated with this method is compared with that of Uspenskii and with that measured by Daniels *et al.* [20], finding a better agreement with experiments than Uspenskii [21], especially at low energies. Still some discrepancies remain. The latter approach [23], developed in the **kp** formalism, allows the calculation of the full optical matrix of Pt and Pd. The energy range is extended up to 100 eV and a substantial reduction of the absorption intensity in the far UV region is found.

We will show below that our calculated EELS spectrum, although neglecting local filed effects, agrees quite well with the experiments over an energy range midway between that of references [22,23]. Besides, it does not present, even for the smallest basis set, the "pathology" at low energy found in the spectrum by Uspenskii [21] and improves also with respect to Fehrenbach's results.

We briefly recall in Section 2 some features of the FP-LMTO method, relevant to the present discussion. More details are to find in references [6,7]. The results of our calculations are discussed in Section 3 and compared with experiments in Section 4. The conclusions are drawn in Section 5.

2 Method of calculation

The FP-LMTO code is based on a variational method where the space is divided, as in the cellular method, in non overlapping so-called muffin-tin (MT) spheres and in the interstitial region, surrounding the spheres. The Kohn-Sham equations have different solutions within the spheres and in the interstitial region. These solutions are then matched at the sphere boundary, *i.e.* at the MT radius S, in a continuous and differentiable way, forming the muffin tin orbital (MTO) $\phi_t(\mathbf{r}-\tau)$ centered on the atom sitting at the sphere center τ. Subscript t includes all the quantum numbers characterizing an atomic-like state: n, l, m, *i.e.*, principal, orbital and magnetic quantum number, plus the *tail* parameter κ^2 described below. The MTO's are the basis functions, atomic-like inside the MT spheres. Outside, they are given by linear combinations of Hankel or Neuman functions. The latter ones, also called *tails* or envelope functions, have kinetic energy κ^2 (negative or positive). The trial wave-function is then expressed as a linear combination of Bloch sums of muffin-tin orbitals: the number of MTO's to be included in the trial function depends, of course, on t, *i.e.*, on n, l, m and on the number of tails κ^2. Core and valence states (here valence states indicate all non-core atomic states, including empty ones) are treated separately in so far the former ones are obtained as exact solution of the Dirac equation with the spherical part of the muffin tin potential. Core charge components may, however, spill out of the parent MT spheres. This contribution ("core leakage") is added to the other valence MT and interstitial charge in the construction of the potential at each step of the self-consistency cycle. In this scheme the truncation of the basis set consists in limiting the number of states included in the trial function. The minimum set nlm of valence basis functions must include the atomic-like states that describe the chemical valence. At least one single tail is then attached to each set of nlm. However, in most calculations, especially in those dealing with optical properties, one must increase this minimum set substantially. This is done by increasing the set of nlm states, *e.g.* by promoting the highest lying core levels into the valence set (semi-core states) and/or adding higher empty valence states. Moreover, more tails for each one of these sets may be used to increase the variational freedom of the basis (multiple κ basis set).

In the present case we include all states in a single fully hybridizing basis, consisting of different sets of nlm with multiple κ^2 to test the convergence of the optical functions with respect to the completeness of the MTO basis. Optical transitions from core states are not considered in our calculation of the dielectric function: this means that the inclusion of semi-core states into the valence set increases the number of possible optical transitions. We remind that our calculations do not include local field effects.

3 Results

The atomic configuration of Pd is [Kr]$4d^{10}5s^0$ and the f.c.c. lattice constant is taken $a = 7.353$ a.u. We perform self-consistent calculations for two groups of MTO's without and with the semicore states $(4s^2, 4p^6)$, respectively. The following sets of quantum numbers describe the valence MTO's for five different basis sets: 1) $2 \times (4d, 5s, 5p, 5d)$, 2) $2 \times (4d, 5s, 5p, 5d, 4f)$, 3) $2 \times (4s, 4p, 4d, 5s, 5p)$, 4) $2 \times (4s, 4p, 4d, 5s, 5p, 5d, 4f)$, 5) $2 \times (4s, 4p, 4d, 5s, 5p, 5d, 6s, 6p, 6d, 4f)$. They correspond to bases of 28, 42, 26, 50, 68 MTO's, respectively. Sets 1 and 2 have the [Kr] configuration in the core whereas sets 3-5 treat also the semi-core states $(4s, 4p)$ as valence state. The factor 2 in front of each bracket means that a twofold of different tails κ^2 is taken for each set with the same nlm. We list in Table 1, for each basis set, the quantum numbers n and l and the values of k^2. The numerical accuracy for integrations in the reciprocal space is achieved by using a regular mesh of 47 k-points in the irreducible wedge of the Brillouin Zone (BZ) with a Gaussian smearing of 2 mRy for the convergence of the potential. 724 k-points in the irreducible wedge of the BZ with the Tetrahedron Method [24] are used to calculate the dielectric function. This turned out to be a good recipe also for bulk Cu and Ag. A preliminary test of convergence is that of the total energy with respect to the muffin-tin radius S. This is a variational parameter that affects the convergence only through the dependence of the MTO's on S (matching at the MT sphere boundary). The optimum choice of S minimizes the total energy. However, its value becomes immaterial for a well converged basis set. In the present case we make the further step of requiring also the convergence of the dielectric function with S, since the eigenfunctions depend on S and affect the optical matrix elements strongly. For metals, the dielectric function contains an intraband (D, stays for Drude) and an interband (i) contribution:

$$\epsilon(\omega) = \left(\epsilon_1^D + \epsilon_1^i\right) + \mathrm{i}\left(\epsilon_2^D + \epsilon_2^i\right) \qquad (1)$$

where the subscripts $1, 2$ in the above equation denote the real and imaginary parts of the dielectric function $\epsilon(\omega)$. The interband term ϵ_2^i is computed *ab initio* and is the one whose convergence we want to test. The real part ϵ_1^i is obtained by Kramers-Kronig transform from ϵ_2^i with a broadening of 0.01 eV. The Drude terms are calculated by the well-known relations [16] $\epsilon_1^D = 1 - \frac{\omega_p^2\tau^2}{1+\omega^2\tau^2}$ and $\epsilon_2^D = \frac{\omega_p^2\tau}{\omega(1+\omega^2\tau^2)}$, with $\hbar\omega_p = 3$ eV and a relaxion time $\frac{\tau}{\hbar} = 8.5\ \mathrm{eV}^{-1}$ deduced from measurements [17].

We focus on sets 1) and 2), without semi-core states, and perform calculations for two different values of the MT radii S_1, S_2 such that the ratio $2S/d = 96\%, 98\%$, respectively, where d is half the first nearest neighbour distance. We first notice that, within each basis set 1) and 2) the total energy, obtained with S_1 and S_2, coincides within 1 mRy. However, set 2) gives a total energy lower by roughly one hundredth of a Ry compared to set 1). Thus, as far as the total energy is concerned, either MT radius satisfies the convergence criterium for either basis set 1 and 2.

Table 1. Quantum numbers n, l and k^2 value (in Ry) for the basis sets 1-5 described in the text.

Basis set	n	l	k^2
1	4	2	$-0.2, +0.5$
	5	0	$-0.2, +0.5$
	5	1	$-0.2, +0.5$
	5	2	$-0.8, +0.2$
2	4	2	$-0.2, +0.5$
	5	0	$-0.2, +0.5$
	5	1	$-0.2, +0.5$
	5	2	$-0.8, +0.2$
	5	3	$-0.2, +0.5$
3	4	0	$-5.5, -2.5$
	4	1	$-1.5, -0.5$
	4	2	$-0.5, +0.2$
	5	0	$+0.2, +0.5$
	5	1	$+0.2, +0.5$
4	4	0	$-5.5, -2.5$
	4	1	$-1.5, -0.5$
	4	2	$-0.5, +0.2$
	4	3	$+0.2, +0.5$
	5	0	$+0.2, +0.5$
	5	1	$+0.2, +0.5$
	5	2	$+0.2, +0.5$
5	4	0	$-5.5, -2.5$
	4	1	$-2.5, -1.5$
	4	2	$-0.5, +0.2$
	4	3	$+1.5, +4.5$
	5	0	$-0.5, +0.2$
	5	1	$-0.5, +0.2$
	5	2	$+0.2, +1.5$
	6	0	$+1.5, +4.5$
	6	1	$+1.5, +4.5$
	6	2	$+1.5, +4.5$

We have then calculated ϵ_2^i for each of the two basis sets with S_1 and S_2. The plot in Figure 1 indicates that only for the basis set 2, the choice of the MT radius is practically immaterial also at the highest energies where basis truncation effects become more important. We henceforth fix S=S_2 in all further calculations. For the discussion of the convergence of the dielectric function with respect to the completeness of the basis we plot in Figures 2a and b ϵ_2 and ϵ_1, respectively, for the five basis sets of MTO's given above. The first thing to notice is that the curves for the five basis sets split into two groups according to whether they contain the $4f$ states or not. The inclusion of the f states in the basis set introduces sizeable differences in the narrow interval 0–2 eV, in ϵ_1 and ϵ_2 and also over the rest of the spectrum beyond about 5 and 10 eV. The convergence of the sets 2, 4, 5, with the $4f$ states, is quite good over the whole range except at the very end of the spectrum as can be clearly seen in the insets of Figures 2a, b. From about 35 eV in ϵ_2 and 32 eV in ϵ_1 (see the insets of Figures 2a and b, respectively), the slope of the

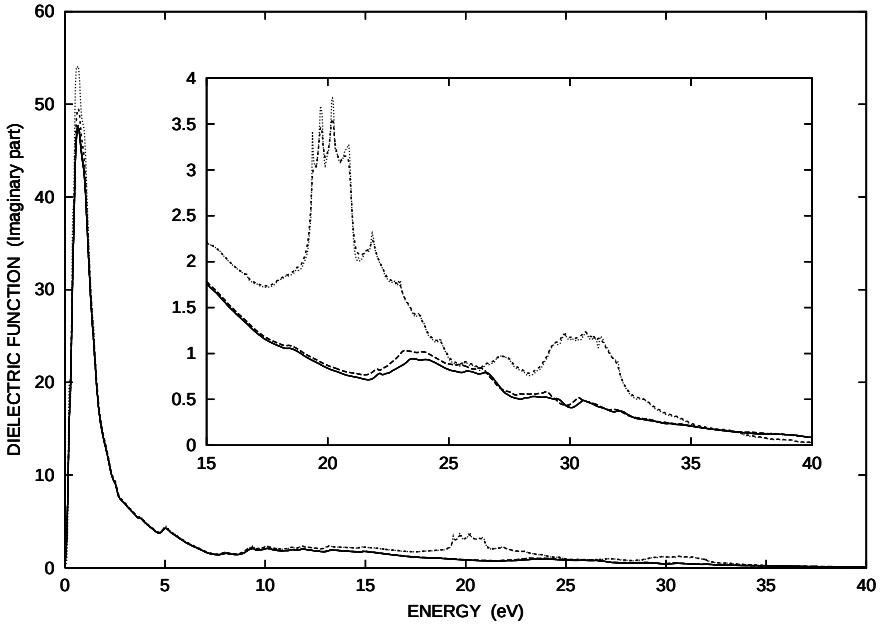

Fig. 1. Imaginary part of the interband dielectric function ϵ_2^i calculated for the basis sets 1 and 2 for two different values of the muffin-tin radius S_1 and S_2. Set 1: S_1 continuous, S_2 dashed; Set 2: S_1 short-dashed, S_2 dotted. The plot in the inset has the same symbols.

curves relative to set 2) *vs.* sets 4), 5) changes. We ascribe this difference to the simultaneous presence of semi-core states and f states in the sets 4) and 5), which makes transitions at higher energies possible. From the inset of Figure 2a we see that ϵ_2 is vanishing for the less complete sets and not for the most complete ones at the highest energies. This indicates that electronic states available to optical transitions are possibly present beyond 40 eV. We shall consider this point carefully in the next section when comparing with the experimental results. Now, as far as the completeness of the basis is concerned, we conclude that the dielectric function is converged up to 30 eV if the basis contain $4f$ valence states and up 40 eV when also semi-core $4s, 4p$ states are furher included. The results obtained with sets 4) and 5) are very similar to each other everywhere; this means that including $6s, 6p$ and $6d$ states in the basis is not crucial. We observe, in passing, that inspection of the wavefunctions show that sets 3), 4) and 5) with semi-core states give a negligeable "core leakage" with respect to the sets 1) and 2), in better agreement with the ideal representation of core states.

We now want to see how the differences in $\epsilon(\omega)$ affect the EELS spectrum. The energy loss function, without local fields, is given by:

$$-\mathrm{Im}(\epsilon^{-1}) = \frac{\epsilon_2}{\epsilon_1^2 + \epsilon_2^2}. \qquad (2)$$

We plot in Figure 3 $-\mathrm{Im}(\epsilon^{-1})$ for the five sets of MTO's above. Also in this case, as in Figure 2, there is a split of the curves relative to the MTO's with and without $4f$ states. We can, in this case, clearly distinguish three different regimes. At low energy (<7 eV) all the basis sets give the same result. Hencefort up to about 34 eV the three sets with the f states are almost indistinguishable. After this energy sets 4) and 5) split from 1), 2), 3). In particular, the unphysical high peak at 36 eV for set 2) is strongly smoothed out in sets 4) and 5). We notice that sets including semi-core states (3, 4, 5) have a positive slope at the very end of the spectrum. At the light of these results we conclude that all sets give a converged EELS spectrum below 7 eV, $4f$ electrons must be included to increase the convergence up to 34 eV and semi-core $4s, 4p$ states are needed to push the convergence up to 40 eV.

Basis sets 1) and 3), which include 23 or less empty states, yield discrepancies with respect to the more complete basis sets of the order of 50% around 20 eV. This is in agreement with a similar error found by Fehrenbach when employing about 30 empty states [22]. He finds that about 500 empty bands are needed to get 1% accuracy in the response function. In the present work $\simeq$60 empty bands are enough to get an accuracy of about 10%. We think that, in view of the neglection of many-body effects in the calculations (self-energy and electron-hole interaction effects in both, also local field effects in ours), a better accuracy is not worth.

4 Comparison with experiments

Several optical functions of the transitions and noble metals, among which Pd, have been measured in an energy range between 0 and 30 eV [16–18] whereas the electron energy loss has been measured up to 70 eV by Daniels *et al.* [19,20]. We notice that the comparison of the measured dielectric function [16] with that obtained by our calculations (see Fig. 2) up to 40 eV is very satisfactory.

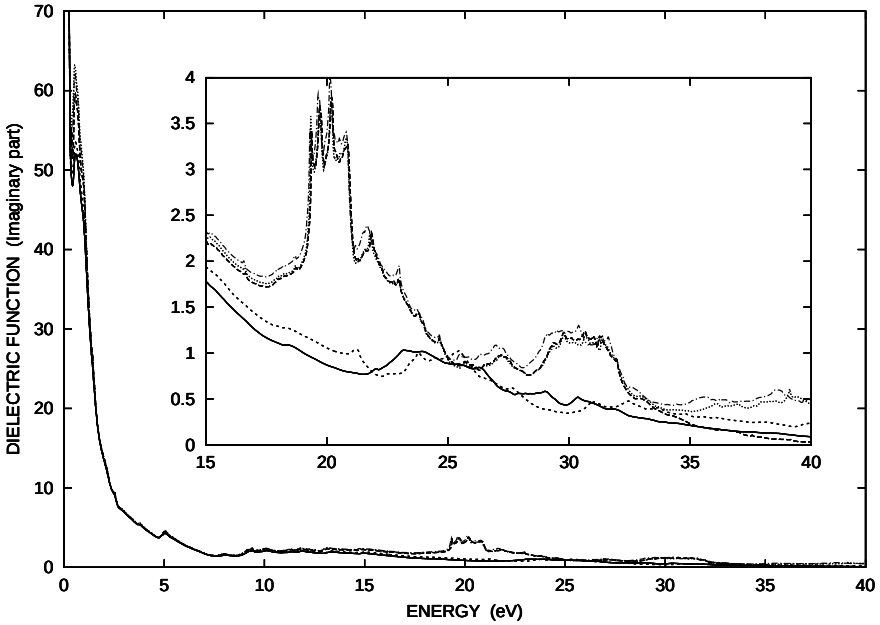

(a)

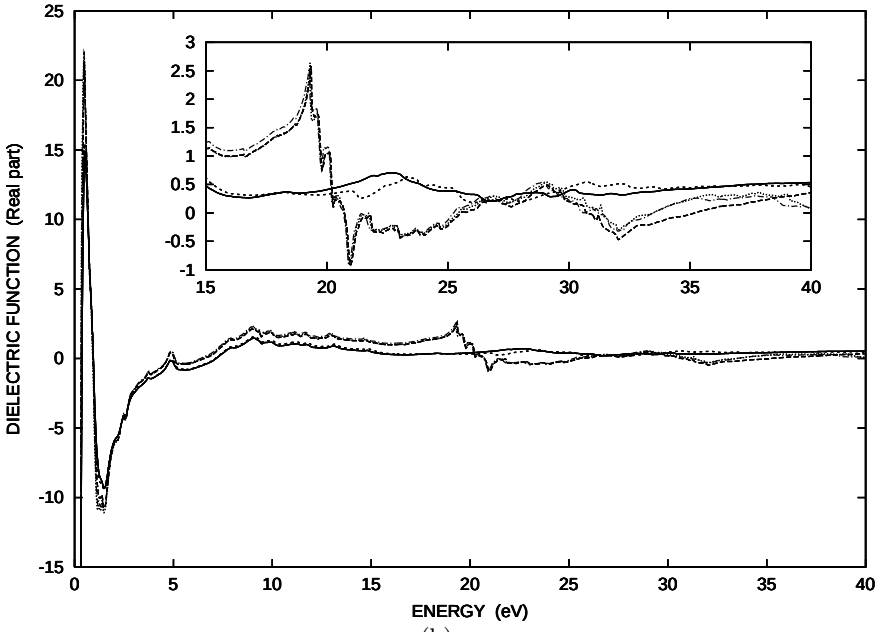

(b)

Fig. 2. Imaginary (a) and real (b) part of the dielectric function calculated for the five different basis sets described in the text: set 1) continuous, set 2) dashed, set 3) short-dashed, set 4) dotted, set 5) dot-dashed line.

We are, however, interested in comparing the EELS, equation (2), with that measured up to 70 eV. For this reason we have tried to extend the calculation of ϵ_2 to higher energies to increase the accuracy of the Kramers-Kronig transform and to allow a comparison over the whole experimental range. This has been obtained in two steps. First we have extended the *ab initio* calculation of ϵ_2^i up to 70 eV. Then we have increased the range of the dielectric function up to 1000 eV by merging the calculated $\epsilon_2(\omega)$ with a smooth, monotonic curve obtained, as common practice, using the optical parameters of Henke *et al.* [25]. The two curves must be matched at an energy value after which the features in the calculated ϵ_2 may be neglected. In Figure 4 we have plotted ϵ_2^i from the raw calculation

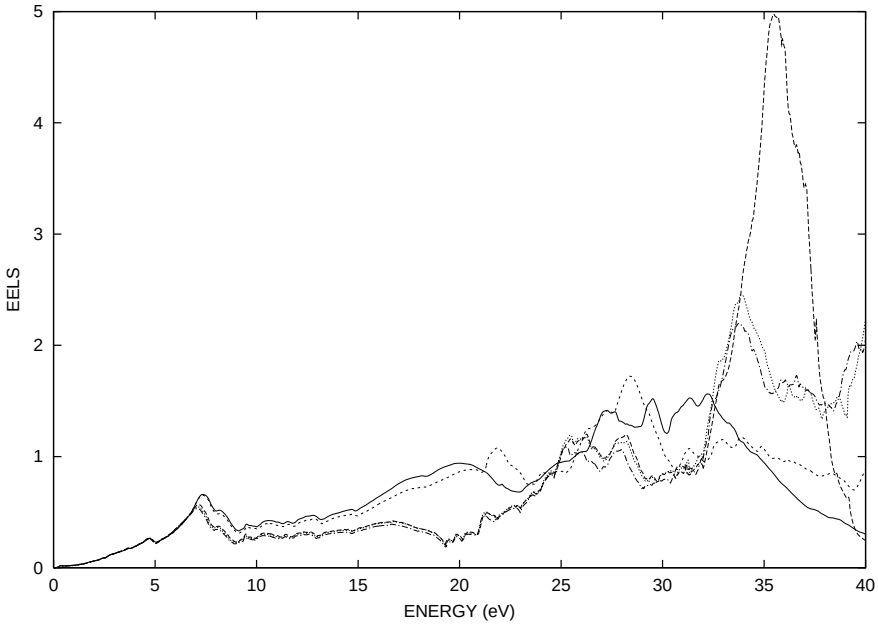

Fig. 3. Spectrum of the loss function calculated from the dielectric functions plotted in Figure 2 with the same symbols.

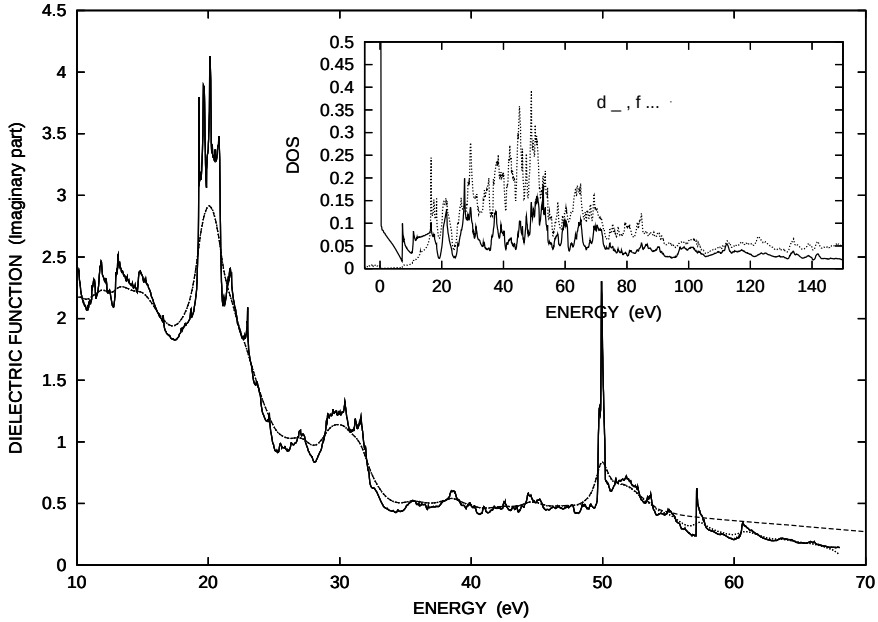

Fig. 4. Imaginary part of the interband dielectric function of Pd obtained without (continuous), with (dotted) a broadening of 0.5 eV, and with a semi-empirical prolongement and a broadening of 0.5 eV (dashed). In the inset are plotted the d (continuous) and f (dotted) partial densities of states.

(continuous), with a broadening of 0.5 eV (dashed) and with the "queue" attached at 55.4 eV (dotted) since optical transitions still occur at 50 eV. By inspection of the partial d and f density of states (DOS) in the inset of Figure 4 we see that the high energy peaks are ascribable to transitions from occupied d states, just below zero (the Fermi level), to f empty states, whose density of states peaks around 50 eV (s and p components are completely negligible here). After this energy, due to the gradual vanishing of the density of states and matrix elements, optical transitions become much less intense.

The curve of the energy loss function calculated with the extended dielectric function is plotted in Figure 5 along with two different experimental spectra [19,20] and results of previous calculations. We report in panel (a) the experimental data of reference [20], where the transmitted electrons are scattered by a small, though non vanishing, angle < 1 mrad. We estimate that in this case the

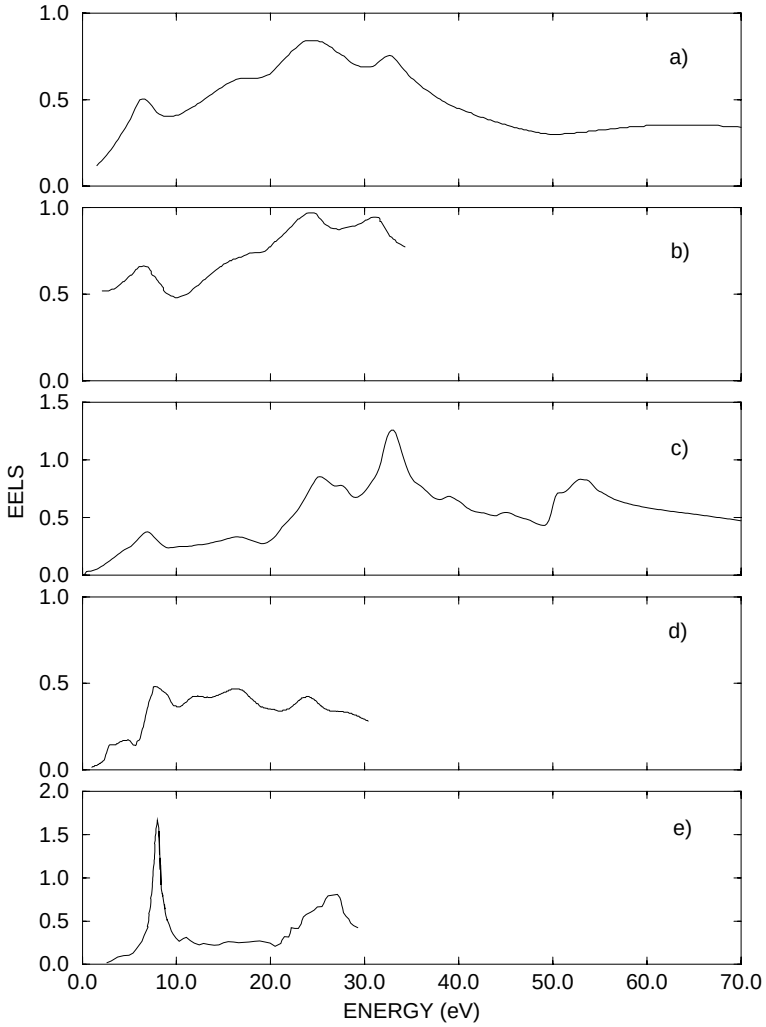

Fig. 5. Loss function of Pd: a) experiment of reference [20] carried out at non zero scattering angle; b) experiment of reference [19] carried out at vanishing scattering angle; c) present calculation; d) calculation from reference [22]; e) calculation from reference [21].

momentum transfer is not negligible, of the order of half the Brillouin Zone boundary, *i.e.* too large for the dipole approximation to be valid as assumed throughout in our calculations. Therefore, the comparison between theory and the plot in panel (a) can be only qualitative, at least at low energy, where the scattering angle affects the intensity [19]. In panel (b) we plot the curve from reference [19] obtained at zero scattering angle, thus fulfilling our zero momentum assumption, but in a shorter energy range up to 30 eV. In fact the agreement of our results, plotted in panel (c), is rather good: the positions of peaks and dips are practically coincident among theory and measurements. At energies beyond those of panel (b), the agreement with the curve in panel (a) can be still considered reasonable between 35–50 eV. In fact the slope is monotonically decreasing in both curves, and after 50 eV where the experimental curve shows a weak but sizeable upturn reminiscent of the peak in the theoretical curve. The fact that experimental structures become weaker than the calculated ones at higher energies can be easily explained in terms of increasing life-time broadening of the relevant excitations.

In Figure 5 we also report the energy loss spectra of Pd, as calculated by Fehrenbach [22] (panel (d)), and by Uspenskii [21] (panel (e)). We notice that these previous theoretical results were obtained for a smaller energy range than in our present calculations. The agreement of these two theoretical curves with the experimental one in panel (b) is worse than in our case (see the high peak at $\simeq$7 eV in the calculation of Uspenskii and the structure around 12 eV in the calculation of Fehrenbach). In particular, we think that the "pathologically" high peak found by Uspenskii, is due to an insufficient sampling of the Brillouin Zone in the numerical integrations rather

than to an intrinsic deficiency of the LMTO-ASA method, as speculated by Fehrenbach [22].

5 Conclusions

We found that the FP-LMTO method is appropriate to calculate optical functions of transition metals and tested this method against the range of energy where the energy loss function of Pd may be calculated to be in good agreement with experiments. The quantitative accuracy of the calculations is completely controlled by the completeness of the MTO's basis functions and by the energy interval in which the interband dielectric function is calculated. Since the increase of the basis set is computationally very easy to achieve and the energy range may be extended to a value comparable to that of experiments, the FP-LMTO turns out to be very appropriate to determine *ab initio* optical properties in so far DFT-LDA is applicable. The number of empty bands included in the calculations needed to obtain converged results depends on the energy range of interest. This is rather obvious, since including more empty bands results in considering more high energy transitions. We found that a reasonable convergence in the loss function up to 70 eV is achieved using about 60 empty bands. The quantitative agreement of our results with experiments supports these conclusions.

We are grateful to J.M. Wills for supplying the FP-LMTO code used in this work and to O. Eriksson for helpful discussions. P.M, R.D.S. acknowledge the support of the following funding agencies: INFM (PRA 1MESS and Parallel Computing Initiative), MURST (COFIN 1999), CNR.

References

1. P. Hohenberg, W. Kohn, Phys. Rev. B **136**, 864 (1964); W. Kohn, L.J. Sham, Phys. Rev. B **140**, 1133 (1965).
2. see, for instance, R.E. Van Camp, V.E. Van Doren, J.T. Devreese, Phys. Rev. B **38**, 12675 (1988).
3. see, for instance, F. Bechstedt, R. Del Sole, Phys. Rev. B **38**, 7710 (1988).
4. A. Continenza, P. Monachesi, M. Galli, F. Marabelli, E. Bauer, Physica Scripta T **66**, 177 (1996).
5. P. Monachesi, Z. Domanski, M.S.S. Brooks, Phys. Rev. B **50**, 1013 (1994).
6. J. Wills, B.R. Cooper, Phys. Rev. B **36**, 3809 (1987); M. Springborg, O.K. Andersen, J. Chem. Phys. **87**, 7125 (1987); M. Methfessel, Phys. Rev. B **38**, 1537 (1988); S. Savrasov, D. Savrasov, Phys. Rev. B **46**, 12181 (1992).
7. O.K. Andersen, Phys. Rev. B **12**, 3060 (1975); H.L. Skriver, *The LMTO method* (Springer-Verlag, Berlin 1984).
8. P. Monachesi, M. Palummo, R. Del Sole, R. Ahuja, O. Eriksson, Mat. Res. Soc. Symp. Proc. **579**, 50 (2000).
9. S.L. Adler, Phys. Rev. **126**, 413 (1962); N. Wiser, Phys. Rev. **129**, 62 (1963).
10. H. Ehrenreich, M.L. Cohen, Phys. Rev. **115**, 786 (1959).
11. W. Hanke, Adv. Phys. **27**, 287 (1978).
12. F. Bassani, G. Pastori Parravicini, *Electronic States and Optical Transitions in Solids*, edited by R.A. Ballinger (Pergamon Press, Oxford 1975), p. 154.
13. M. Alouani, J.M. Wills, Phys. Rev. B **54**, 2480 (1996).
14. R. Ahuja, A. Auluk, J.M. Wills, M. Alouani, B. Johansson, O. Eriksson, Phys. Rev. B **55**, 4999 (1997).
15. A. Marini, G. Onida, R. Del Sole, Phys. Rev. B **64**, 195125 (2001).
16. P.B. Johnson, R.W. Christy, Phys. Rev. B **9**, 5056 (1974).
17. J.H. Weaver, R.L. Benbow, Phys. Rev. B **12**, 3509 (1975).
18. J.H. Weaver, Phys. Rev. B **11**, 1416 (1975).
19. J. Daniels, Z. Physik **277**, 234 (1969).
20. J. Daniels, C.v. Festenberg, H. Raether, K. Zeppenfeld in *Optical Constants of Solids by Electron Spectroscopy*, edited by G. Höler Springer Tracts in Modern Physics, Vol. 54 (Springer, Berlin, 1970), p. 77.
21. Y.A. Uspenskii, E.G. Maximov, S.N. Rashkeyev, I.I. Mazin, Z. Physik B **53**, 263 (1983); I.I. Mazin, E.G. Maximov, S.N. Rashkeyev, Y.A. Uspenskii, in *Metal Optics and Superconductivity* (Nova Science, New York, 1991).
22. G.M. Fehrenbach, Phys. Rev. B **59**, 15085 (1999).
23. E.E. Krasovskii, W. Schattke, Phys. Rev. B **63**, 235112 (2001).
24. O. Jepsen, O.K. Andersen, Solid State Comm. **9**, 1763 (1971).
25. B.L. Henke, E.M. Gullikson, J.C. Davis, in *Atomic Data and Nuclear Data Tables*, Vol. 54, 2 pp. 181–342 (1993).